

## Amide–Amine Replacement in Indole-2-carboxamides Yields Potent Mycobactericidal Agents with Improved Water Solubility

Yu Jia Tan,<sup>‡</sup> Ming Li,<sup>‡</sup> Gregory Adrian Gunawan, Samuel Agyei Nyantakyi, Thomas Dick, Mei-Lin Go,\* and Yulin Lam\*Cite This: <https://dx.doi.org/10.1021/acsmchemlett.0c00588>

Read Online

ACCESS |



Metrics &amp; More



Article Recommendations



Supporting Information

**ABSTRACT:** Indolecarboxamides are potent but poorly soluble mycobactericidal agents. Here we found that modifying the incipient scaffold by amide–amine substitution and replacing the indole ring with benzothioephene or benzoselenophene led to striking (10–20-fold) improvements in solubility. Potent activity could be achieved without the carboxamide linker but not in the absence of the indole ring. The indolylmethylamine, *N*-cyclooctyl-6-trifluoromethylindol-2-ylmethylamine (**33**, MIC<sub>90Mtb</sub> 0.13 μM, MBC<sub>99.9Mtb</sub> 0.63 μM), exemplifies a promising member that is more soluble and equipotent to its carboxamide equivalent. It is also an inhibitor of the mycolate transporter MmpL3, a property shared by the methylamines of benzothioephene and benzoselenophene.

**KEYWORDS:** Mycobactericidal activity, indolylmethylamines, MmpL3, water solubility

Compound 16		Compound 33	
MIC <sub>90 Mtb</sub>	0.04 μM	MIC <sub>90 Mtb</sub>	0.13 μM
MBC <sub>99.9 Mtb</sub>	0.08 μM	MBC <sub>99.9 Mtb</sub>	0.63 μM
Vero IC <sub>50</sub>	> 100 μM	Vero IC <sub>50</sub>	22 μM
Solubility (pH 7.4)	2.2 μM	Solubility (pH 7.4)	31 μM
PAMPA P <sub>e</sub>	0.34 × 10 <sup>-6</sup> cm/s	PAMPA P <sub>e</sub>	13.4 × 10 <sup>-6</sup> cm/s
Microsomal T <sub>1/2</sub>	25.6 min	Microsomal T <sub>1/2</sub>	8.2 min

Tuberculosis (TB) is a preventable and treatable disease caused by the organism *Mycobacterium tuberculosis* (*M. tb*). Global eradication of TB is hampered by onerous treatment regimens, prevalence of recalcitrant mycobacteria and widespread asymptomatic latent infections that can escalate to the active, transmissible disease.<sup>1</sup> In 2019, there were 10 million cases of TB and 1.2 million deaths (non-HIV) worldwide.<sup>1</sup> Transmission rates have slowed but not changed significantly over the years, and TB remains a leading cause of death attributed to a single infectious agent. Clearly, there is an urgent need for greater global commitment to TB eradication and more potent, faster-acting, and nontoxic drugs to support these efforts.

Exploration of the indole-2-carboxamide scaffold for mycobactericidal activity has yielded several potent lead compounds (**1–7**, Figure 1).<sup>2–8</sup> The *N*-adamantyl analog **1** was short-listed from an extensive screening exercise, which triaged compounds for bactericidal potencies, drug-like physicochemical properties, and selective toxicities.<sup>3</sup> In another investigation, optimization of initial hits led to the *N*-(4,4-dimethylcyclohexyl)indolecarboxamides **2** and **3**, which displayed potent activity against *M. tb*, impressive safety profiles, and *in vivo* activity.<sup>2,4</sup> Potent activities were also detected in disubstituted indolecarboxamides bearing cyclooctyl (**4**), trimethylbicyclo[3.1.1]heptanyl (**5**), and spiro[5.5]-undecanyl (**6**) rings at the amide N.<sup>5–8</sup> Evidence from genetic, crystallographic, and biochemical investigations point to the essential mycolic acid transporter MmpL3 as the putative target of several indolecarboxamides,<sup>4,6,9</sup> with affinity largely

driven by the hydrogen (H) bonding carboxamide and hydrophobic rings within the scaffold.<sup>9</sup>

In spite of their exceptional bactericidal potencies, the translational potential of the indolecarboxamides is impeded by limited aqueous solubilities.<sup>2,3,8</sup> Poor solubility is predicated on the structure–activity requirement for hydrophobic residues and H bonding groups (indole NH, amide carbonyl). Hydrophobic structures increase lipophilicity, while the proximity of H bond donor and acceptor residues in the scaffold promote intramolecular H bonding.<sup>10</sup> We posited that measured efforts at attenuating either or both features could enhance solubility without incurring disproportionate losses in antibacterial activity. The lipophilicity of indolecarboxamides may be diminished by exploring monosubstitution as an alternative to disubstitution, which has been the preferred approach.<sup>2,4–8</sup> Disruption of H bonding could be effected by (i) replacing the indolyl NH (H bond donor) with sulfur or selenium, thereby generating novel functionalized benzothioephene and benzoselenophene, or (ii) removing the H bonding amide carbonyl, hence converting the carboxamide to a protonatable amine. Conversion to the amine as seen in 7

**Special Issue:** RNA: Opening New Doors in Medicinal Chemistry

**Received:** November 7, 2020

**Accepted:** November 11, 2020

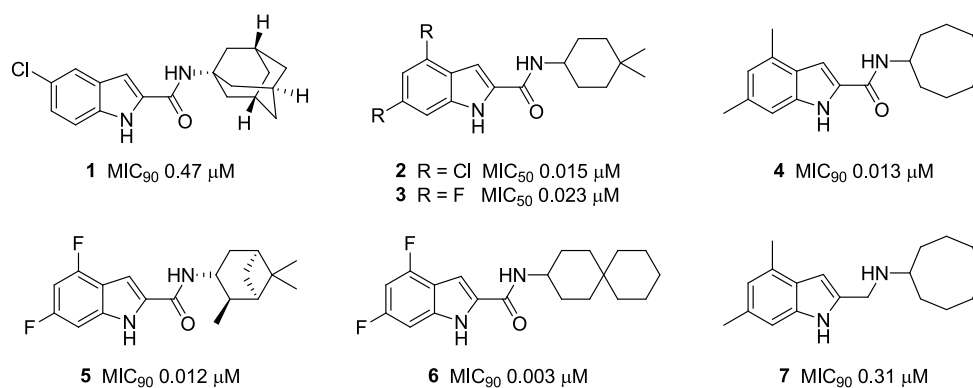


**Figure 1.** Structures and minimum growth inhibitory concentrations (MICs) of indolecarboxamides (1–7) against *M. tb* H37Rv. MIC<sub>90</sub> values were not cited for 2 and 3.<sup>2</sup>

**Table 1.** *M. bovis* BCG Growth Inhibitory MIC<sub>90</sub> Values (μM) and log *D* (pH 7.4) of Series I and II

Series I									
No.	R <sup>1</sup>	R <sup>2</sup>	Log <i>D</i> <sup>a</sup>	MIC <sub>90</sub> (μM) <sup>b</sup>	No.	R <sup>1</sup>	R <sup>2</sup>	Log <i>D</i> <sup>a</sup>	MIC <sub>90</sub> (μM) <sup>b</sup>
4 <sup>c</sup>	4,6-CH <sub>3</sub>	Cyclooctyl	5.42	0.04	16	6-CF <sub>3</sub>	Cyclooctyl	5.57	0.04
8	H	Cyclooctyl	4.86	0.52	17	5-OMe	Cyclooctyl	4.36	0.65
9	5-F	Cyclooctyl	4.91	0.61	18	6-OMe	Cyclooctyl	4.35	1.1
10	6-F	Cyclooctyl	5.05	0.18	19	5-OH	Cyclooctyl	3.76	48
11	5-Cl	Cyclooctyl	5.35	0.80	20	6-OH	Cyclooctyl	4.42	11
12	6-Cl	Cyclooctyl	5.68	0.11	21	5-OBn	Cyclooctyl	5.66	0.17
13	5-Br	Cyclooctyl	5.06	1.1	22	6-OBn	Cyclooctyl	5.65	0.07
14 <sup>c</sup>	6-Br	Cyclooctyl	5.69	0.06	23	6-CF <sub>3</sub>	Cyclohexyl	4.51	1.6
15	5-NO <sub>2</sub>	Cyclooctyl	4.78	0.41	24	6-CF <sub>3</sub>	Cycloheptyl	5.04	0.21
Series II									
No.	R <sup>1</sup>	R <sup>2</sup>	Log <i>D</i> <sup>a</sup>	MIC <sub>90</sub> (μM) <sup>b</sup>	No.	R <sup>1</sup>	R <sup>2</sup>	Log <i>D</i> <sup>a</sup>	MIC <sub>90</sub> (μM) <sup>b</sup>
7 <sup>c</sup>	4,6-CH <sub>3</sub>	Cyclooctyl	2.52	0.25	31	6-Br	Cyclooctyl	2.94	0.16
25	H	Cyclooctyl	2.08	0.75	32	5-NO <sub>2</sub>	Cyclooctyl	2.06	0.69
26	5-F	Cyclooctyl	2.17	0.33	33	6-CF <sub>3</sub>	Cyclooctyl	2.82	0.08
27	6-F	Cyclooctyl	2.31	0.43	34	5-OMe	Cyclooctyl	1.60	1.5
28	5-Cl	Cyclooctyl	2.60	0.22	35	6-OMe	Cyclooctyl	1.59	1.2
29	6-Cl	Cyclooctyl	2.93	0.10	36	5-OBn	Cyclooctyl	2.90	0.31
30	5-Br	Cyclooctyl	2.31	0.74	37	6-CF <sub>3</sub>	Cyclohexyl	1.80	1.1

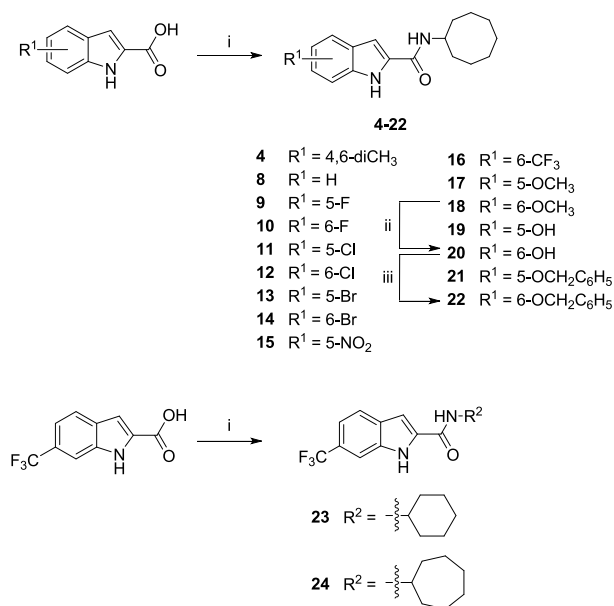
<sup>a</sup>Values of log *D*, pH 7.4, were obtained from ACD /Labs, version 12.01. <sup>b</sup>Lowest concentration required to reduce bacterial growth by 90% compared to untreated cultures. From *n* = 2 separate determinations. MIC<sub>50</sub> and MIC<sub>90</sub> of control isoniazid were 1.6 μM and 3.2 μM. <sup>c</sup>Reported compounds.<sup>7</sup>

(MIC<sub>90</sub> 0.31 μM) admittedly led to lower activity when compared to the carboxamide 4 (MIC<sub>90</sub> 0.013 μM, Figure 1).<sup>7</sup> However, as such amine–amide comparisons are not widely reported, further investigations are warranted. In this report, structural modifications were made with reference to the estimated log *D*<sub>7.4</sub> (5.42, Table 1) of the potent indolecarbox-

amide 4, with the aim that the lipophilicities of our proposed analogs should not exceed this threshold value. To this end, we synthesized the 2-carboxamides of monosubstituted indoles (series I), benzothiophenes (series III), and benzoselenophenes (series V) and the 2-aminomethyl analogs of the same scaffolds (series II, IV, VI).

The series I indole-2-carboxamides (**4**, **8–24**) were synthesized by amide coupling of commercially available indole-2-carboxylic acids with appropriate amines in the presence of 1-ethyl-3-(3-(dimethylamino)propyl)carbodiimide hydrochloride (EDC·HCl), hydroxybenzotriazole (HOBt) and *N,N*-diisopropylethylamine (DIPEA) (Scheme 1). In the case

### Scheme 1. Synthesis of Indole-2-carboxamides (Series I)<sup>a</sup>



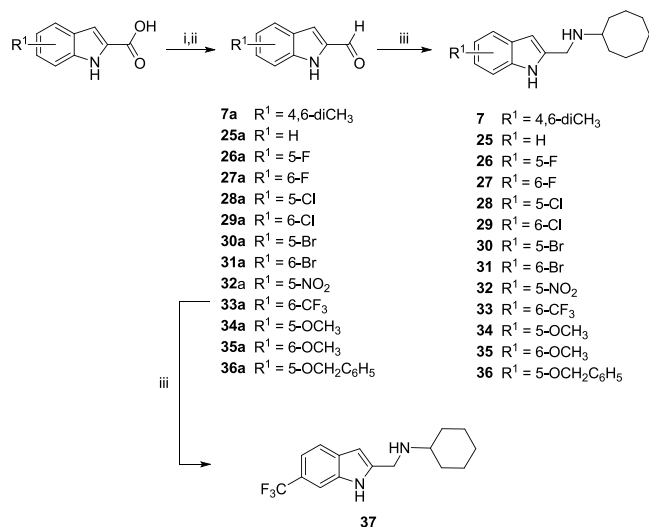
<sup>a</sup>Reagents and conditions: (i) R<sup>2</sup>-amine, EDC·HCl, HOBt, DIPEA, CH<sub>2</sub>Cl<sub>2</sub> or DMF, rt, 3–12 h, 10–76%; (ii) BBr<sub>3</sub>, CH<sub>2</sub>Cl<sub>2</sub>, 0 °C to rt, 12 h, 81%; (iii) benzyl bromide, K<sub>2</sub>CO<sub>3</sub>, DMF, rt, 2 h, 21%.

of **20** and **22** for which carboxylic acid precursors were not available, they were obtained by stepwise demethylation of 6-methoxy in **18** to give the 6-hydroxyl analog **20**, which was then reacted with benzyl bromide to give the 6-benzyloxy derivative **22**.

To obtain series II (Scheme 2), commercially available indolyl-2-carboxylic acids were reduced to the corresponding alcohol with lithium aluminum hydride (LiAlH<sub>4</sub>), and then oxidized to the carbaldehyde with pyridinium dichromate (PDC) or manganese dioxide (MnO<sub>2</sub>). The carbaldehydes (**7a**, **25a–36a**) were subsequently converted to the desired indolylmethylamines (**7**, **25–37**) by reductive amination.

As in series I, amide coupling of benzothioephene-2-carboxylic acid and reductive amination of benzothioephene-2-carbaldehyde were employed to give the non-ring-substituted benzothioephene-2-carboxamides (**39–42**) and benzothioephene-2-methylamines (**45–47**) (Scheme 3A). Note that the *N*-adamantan-1-amino analog **48** was obtained by reducing the precursor carboxamide **42** with LiAlH<sub>4</sub> in the presence of trimethylsilyl chloride (TMSCl) (Scheme 3A).<sup>11</sup> A different route was employed to obtain the ring-substituted benzothioephene-2-carboxamides (**43**, **44**) and 2-methylamines (**49**, **50**) (Scheme 3B). Here, 4-bromo-2-fluorobenzaldehyde and 2-fluoro-4-trifluoromethylbenzaldehyde were reacted with ethyl thioglycolate to give the ethyl esters of 6-substituted benzothioephene-2-carboxylic acids (**43a**, **44a**).<sup>12</sup> Alkaline hydrolysis of the esters followed by amide coupling of the carboxylic acids **43b** and **44b** with cyclooctylamine yielded the

### Scheme 2. Synthesis of Indole-2-methylamines (Series II)<sup>a</sup>



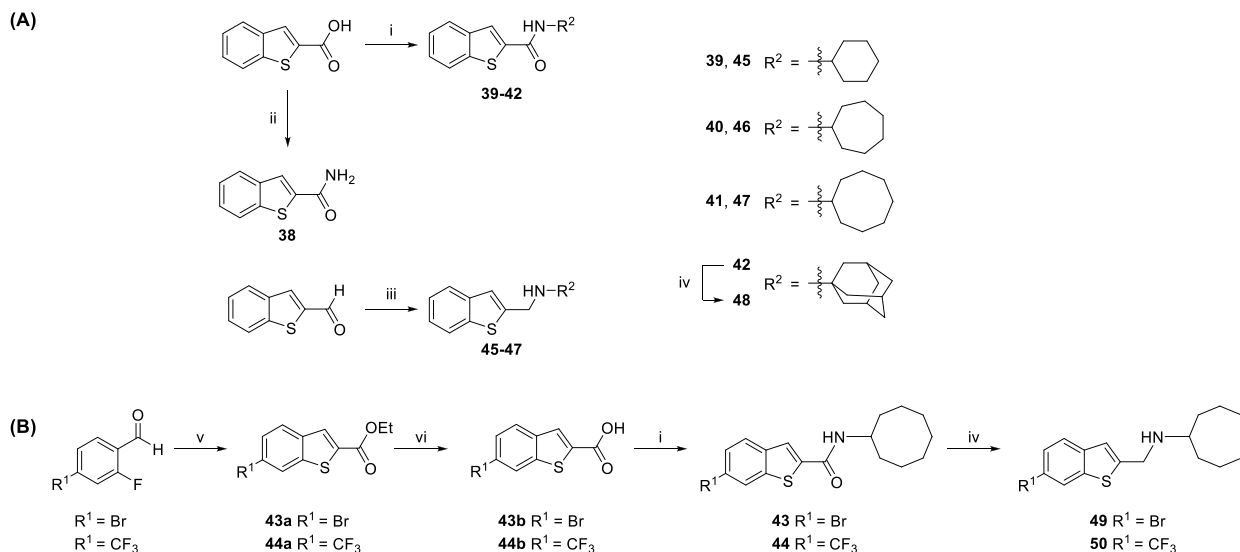
<sup>a</sup>Reagents and conditions: (i) LiAlH<sub>4</sub>, THF, 0 °C to rt, 2–3 h; (ii) PDC, 4 Å molecular sieves or activated MnO<sub>2</sub>, CH<sub>2</sub>Cl<sub>2</sub>, rt, 12 h, 17–54% over two steps; (iii) cyclooctylamine, Na(OAc)<sub>3</sub>BH, acetic acid, THF, rt, 12 h, 10–92%.

*N*-cyclooctyl carboxamides (**43**, **44**), which on LiAlH<sub>4</sub> reduction gave the corresponding methylamines (**49**, **50**).

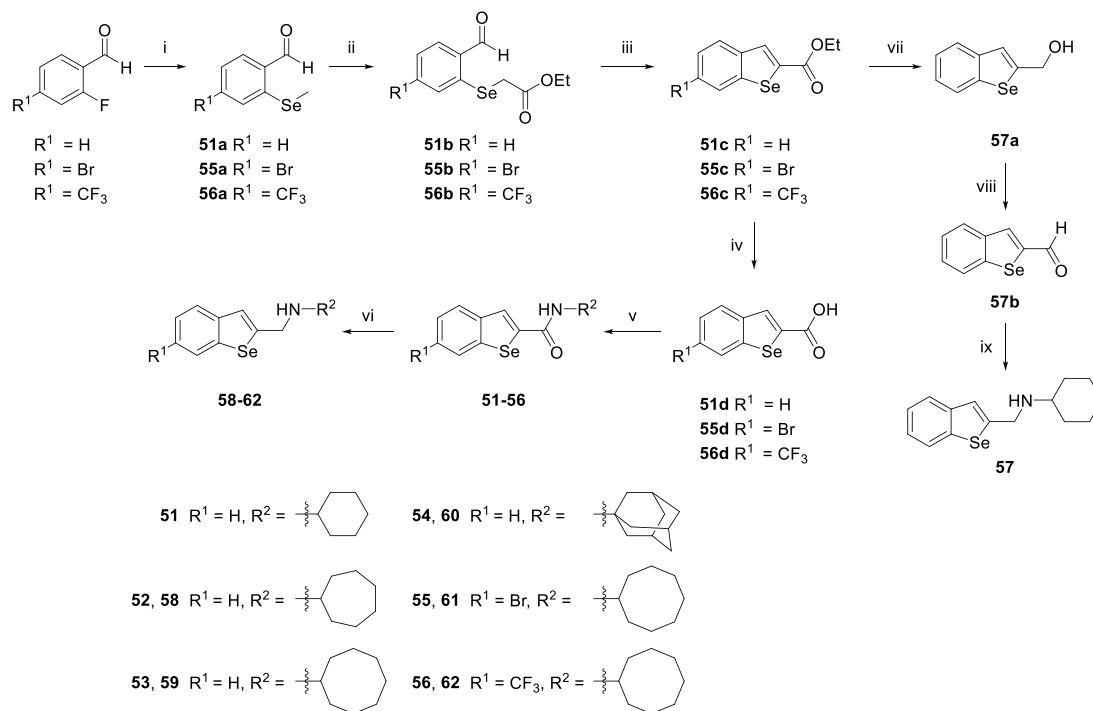
In the case of the benzoselenophenes of series V and VI, the scaffold was synthesized by reacting 2-fluorobenzaldehydes with dimethyldiselenide in the presence of the reducing agent dithiothreitol (DTT) under basic conditions (Scheme 4).<sup>13</sup> Cleavage of the diselenide bond by the nucleophilic thiolate in DTT yielded the negatively charged methylselenoates, which then gave 2-(methylselanyl)benzaldehydes (**51a**, **55a**, **56a**) through fluoride displacement.<sup>14</sup> The nucleophilic selenium in these benzaldehydes reacted with the electron deficient  $\alpha$ -carbon of ethyl bromoacetate with loss of bromide and concurrent demethylation of the methylselanyl side chain to give ethyl 2-[(2-formylphenyl)selanyl]acetates (**51b**, **55b**, **56b**). Aldol reaction led to ring closure and formation of the ethyl esters of benzoselenophene-2-carboxylic acids (**51c**, **55c**, **56c**). Hydrolysis gave the free acids (**51d**, **55d**, **56d**), which on amide coupling yielded the benzoselenophene-2-carboxamides **51–56**. Hydride reduction of the carboxamides yielded most of the series VI benzoselenophenemethylamines (**58–62**) except for the *N*-cyclohexyl analog **57**, which was synthesized by sequential reduction of ester **51c** to the alcohol **57a** and oxidation to the carbaldehyde **57b**, followed by reductive amination.

The MICs of series I–VI compounds were determined by the broth dilution method on *M. bovis* BCG, a mycobacterial model organism. Results are presented in Tables 1 and 2.

Compounds **4** and **14** have been identified as highly potent indolecarboxamides,<sup>7</sup> and here they were resynthesized as positive controls to gauge the potencies of our own compounds. We first examined the growth inhibitory activities of monosubstituted indolecarboxamides (**8–13**, **15–22**) bearing the *N*-cyclooctyl substituent of **4** and **14**. The electron-donating or -withdrawing groups at position 5 or 6 were chosen to ensure that the log *D*<sub>7.4</sub> values of final compounds did not exceed that of **4** (5.42). However, a few compounds (**12**, **16**, **21**, **22**) had marginally higher log *D* values (5.65–5.69) but not exceeding that of **14** (5.69), which

Scheme 3. Synthesis of Benzothiophene-2-carboxamides and Benzothiophene-2-methylamines (Series III and IV)<sup>a</sup>

<sup>a</sup>Reagents and conditions: (i) R<sup>2</sup>-amine, EDC-HCl, HOBt, DIPEA, DMF, rt, 3–12 h, 16–98%; (ii) 25% NH<sub>4</sub>OH, HBTU, Et<sub>3</sub>N, DMF, rt, 30 min, 36%; (iii) R<sup>2</sup>-amine, Na(OAc)<sub>3</sub>BH, acetic acid, THF, rt, 12 h, 15–39%; (iv) LiAlH<sub>4</sub>, TMSCl, THF or CH<sub>2</sub>Cl<sub>2</sub>, 0 °C to rt, 2–6 h, 8–66%; (v) K<sub>2</sub>CO<sub>3</sub>, ethyl thioglycolate, DMF, rt to 60 °C, 22 h, 93–97%; (vi) NaOH, EtOH/H<sub>2</sub>O (1:1), reflux, 1.5 h, 91%–quant.

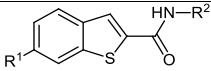
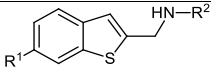
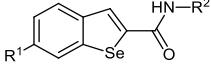
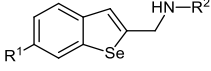
Scheme 4. Synthesis of Benzoselenophene-2-carboxamides and Benzoselenophene-2-methylamines (Series V and VI)<sup>a</sup>

<sup>a</sup>Reagents and conditions: (i) (CH<sub>3</sub>Se)<sub>2</sub>, DTT, DBU, DMF, rt, 1 h, 79%–quant.; (ii) ethyl bromoacetate, 135 °C, 18 h, 90–98%; (iii) K<sub>2</sub>CO<sub>3</sub>, DMF, rt, 24 h, 71–87%; (iv) NaOH, MeOH/H<sub>2</sub>O (9:1), rt, 24 h, 62% for **51d**; NaOH, EtOH/H<sub>2</sub>O (1:1), reflux, 1.5 h, 82–87% for **55d**, **56d**; (v) R<sup>2</sup>-amine, EDC-HCl, HOBt, DIPEA, DMF, rt, 12 h, 60–84%; (vi) LiAlH<sub>4</sub>, TMSCl, THF or CH<sub>2</sub>Cl<sub>2</sub>, 0 °C to rt, 2–6 h, 54–78%; (vii) LiAlH<sub>4</sub>, THF, rt, 2 h, 78%; (viii) PDC, 4 Å molecular sieves, CH<sub>2</sub>Cl<sub>2</sub>, rt, 12 h, 89%; (ix) cyclohexylamine, Na(OAc)<sub>3</sub>BH, acetic acid, THF, rt, 12 h, 19%.

is the other positive control. In all, we found greater potencies among 6-substituted versus 5-substituted regioisomers, with the exception of those with polar methoxy (**17**, **18**) and hydroxy (**19**, **20**) groups. The lipophilic 6-CF<sub>3</sub> analog **16** was the most potent member in series I, with a nanomolar MIC equivalent to **4** and **14**. Hence we posited that growth inhibitory potencies were driven by lipophilicities (log *D*<sub>7,4</sub>),

but this appeared unlikely as no significant correlation (Spearman rho = −0.123, *n* = 32, *p* = 0.502, 2-tailed) was observed when more lipophilic analogs of **21** and **22** (Table S1) were included in the analysis. We then replaced the *N*-cyclooctyl ring in **16** with smaller rings (**23**, **24**) and other variants listed in Table S1. None were comparable to **16**,

Table 2. *M. bovis* BCG Growth Inhibitory MIC<sub>90</sub> Values (μM) and log D (pH 7.4) of Series III–VI

Series III 					Series IV 				
No.	R <sup>1</sup>	R <sup>2</sup>	Log D <sup>a</sup>	MIC <sub>90</sub> (μM) <sup>b</sup>	No.	R <sup>1</sup>	R <sup>2</sup>	Log D <sup>a</sup>	MIC <sub>90</sub> (μM) <sup>b</sup>
38	H	H	2.4	>50	45	H	Cyclohexyl	2.70	>45
39	H	Cyclohexyl	2.88	>50	46	H	Cycloheptyl	3.23	5.0
40	H	Cycloheptyl	3.41	3.0	47	H	Cyclooctyl	3.56	3.4
41	H	Cyclooctyl	3.94	0.50	48	H	1-Adamantyl	3.39	3.6
42	H	1-Adamantyl	3.83	0.90	49	Br	Cyclooctyl	4.51	2.2
43	Br	Cyclooctyl	4.62	0.80	50	CF <sub>3</sub>	Cyclooctyl	4.49	0.78
44	CF <sub>3</sub>	Cyclooctyl	4.65	0.40					
Series V 					Series VI 				
No.	R <sup>1</sup>	R <sup>2</sup>	Log D <sup>a</sup>	MIC <sub>90</sub> (μM) <sup>b</sup>	No.	R <sup>1</sup>	R <sup>2</sup>	Log D <sup>a</sup>	MIC <sub>90</sub> (μM) <sup>b</sup>
51	H	Cyclohexyl	3.77	>50	57	H	Cyclohexyl	2.55	>35
52	H	Cycloheptyl	4.29	2.7	58	H	Cycloheptyl	3.08	5.0
53	H	Cyclooctyl	4.82	0.70	59	H	Cyclooctyl	3.43	2.1
54	H	1-Adamantyl	4.71	1.0	60	H	1-Adamantyl	3.26	2.7
55	Br	Cyclooctyl	5.58	0.78	61	Br	Cyclooctyl	4.43	0.54
56	CF <sub>3</sub>	Cyclooctyl	5.53	1.8	62	CF <sub>3</sub>	Cyclooctyl	4.34	2.0

<sup>a</sup>Values of log D, pH 7.4, were obtained from ACD /Labs, version 12.01. <sup>b</sup>Lowest concentration required to reduce bacterial growth by 90% compared to untreated cultures. From  $n = 2$  separate determinations. MIC<sub>50</sub> and MIC<sub>90</sub> of control isoniazid were 1.6 μM and 3.2 μM.

confirming the widely cited activity advantage associated with the cyclooctyl ring.<sup>2,5,7</sup>

Series II was derived by replacing the carboxamide in series I with a basic and predominantly protonated aminomethyl side chain. Noting that all the series II compounds (7, 25–37) have carboxamide equivalents, we compared potencies across the series. Interestingly, most amide–amine pairs (8 out of 14) were equipotent, with less than 2-fold difference in MIC<sub>90</sub>. Where greater potency was detected, it generally resided in the amide analog (5 out of 6 pairs). Among the series II methylamines, the most potent was the 6-CF<sub>3</sub> analog 33 (MIC<sub>90</sub> 0.08 μM), recapitulating the outstanding activity of its 6-CF<sub>3</sub> counterpart 16 (MIC<sub>90</sub> 0.04 μM) in series I. Replacing the *N*-cyclooctyl ring of 33 with other ring variants (37 and others listed in Table S1) did not benefit activity.

Next, the indole ring in series I was replaced by benzothiophene to give series III (Table 2). To determine if *N*-cyclooctyl was still the favored ring on this scaffold, we replaced it with other carbocycles of different sizes, lipophilicities, and flexibilities in the non-ring-substituted benzothiophene-2-carboxamide (Tables 2, S1). Yet again, the most potent activity resided in the analog with the *N*-cyclooctyl ring (41, MIC<sub>90</sub> 0.5 μM), but here, comparable activity was found in 42 (MIC<sub>90</sub> 0.9 μM), which has the rigid *N*-(1-adamantyl) ring. Lipophilic or bulky carbocycles like 4-*n*-butyl-cyclohex-1-yl, 4-*tert*-butylcyclohex-1-yl, 1-adamantylmethyl, dihydroinden-2-yl were associated with ostensibly weaker activity (MIC<sub>90</sub> 1.5 μM to >50 μM, Table S1). Next, we substituted the benzothiophene ring of 41 with 6-Br (43) and 6-CF<sub>3</sub> (44) as these were the best performing ring

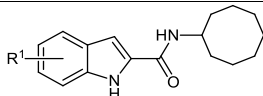
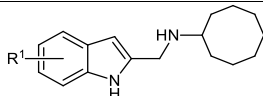
substituents in series I. Disappointingly, 43 and 44 were only equipotent to 41.

The same design approach was applied to the benzothiophene-2-methylamines of series IV (Table 2, Table S1). As in series III, the *N*-cyclooctyl 47 and *N*-(1-adamantyl) 48 were the most potent (MIC<sub>90</sub> 3.5 μM) but significantly less so than their carboxamide counterparts 41, 42 (MIC<sub>90</sub> 0.5, 0.9 μM). Unlike series III, activity rebounded sharply when 47 was substituted with 6-CF<sub>3</sub> (50, MIC<sub>90</sub> 0.78 μM).

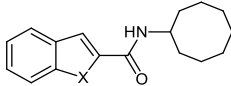
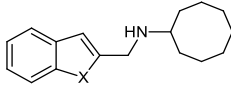
Lastly, we explored the carboxamides (series V) and methylamines (series VI) of benzoselenophene. Here we noted that the MICs of the best performing members in both series (53–55, 61) were broadly comparable to the potent benzothiophenes (41–44, 50). There were also more potent carboxamides than methylamines in both scaffolds. Second, several parallels were noted in the structure–activity relationships of the benzothiophenes (series III, IV) and benzoselenophenes (series V, VI). In the case of the carboxamides (series III, V), the same ring structures (*N*-cyclooctyl, *N*-(1-adamantyl)) were associated with potent activity. MICs of these compounds (41, 42, 53, 54) were also comparable and substitution of the scaffold (6-Br, 6-CF<sub>3</sub>) did not increase potencies. In the case of the methylamines (series IV, VI), the reverse was true. Hence, whereas the non-ring-substituted analogs 47 and 59 displayed modest MICs, a sharp rebound in activity was observed on insertion of 6-Br (50) or 6-CF<sub>3</sub> (61).

Overall, evaluation of our synthesized compounds (Tables 1, 2, S1) showed that indoles were by far the most promising of the three scaffolds and that only the indolylmethylamine 33 was comparable to the most potent indolecarboxamides of

Table 3. Solubility and PAMPA Permeability Profiles of Selected Series I–VI Analogs<sup>c</sup>

							
No.	R <sup>1</sup>	Solubility (μM) <sup>a</sup>	P <sub>e</sub> (10 <sup>-6</sup> cm/s) <sup>b</sup>	No.	R <sup>1</sup>	Solubility (μM) <sup>a</sup>	P <sub>e</sub> (10 <sup>-6</sup> cm/s) <sup>b</sup>
4	4,6-Me	5.7 (0.5)	14.0 (0.8)	7	4,6-Me	70.1 (2.9)	18.4 (1.2)
14	6-Br	1.6 (0.1)	8.1 (1.7)	31	6-Br	35.4 (2.8)	13.4 (1.5)
16	6-CF <sub>3</sub>	2.2 (0.2)	0.34 (0.21)	33	6-CF <sub>3</sub>	31.0 (1.7)	13.4 (1.0)

					
No.	X	Solubility (μM) <sup>a</sup>	No.	X	Solubility (μM) <sup>a</sup>
8	NH	2.4 (0.2)	25	NH	99.7 (3.6)
41	S	3.3 (0.3)	47	S	73.5 (4.1)
53	Se	3.7 (0.4)	59	Se	77.8 (2.2)

<sup>a</sup>Multiscreen filter plates (Millipore), 24 h agitation, pH 7.4, 25 °C. <sup>b</sup>P<sub>e</sub> measures the rate at which a molecule crosses a membrane or lipid bilayer. Multiscreen-IP PAMPA assay donor/receiver plates (Millipore), 1% lecithin in dodecane as barrier, 18 h agitation, pH 7.4, 25 °C. P<sub>e</sub> of propranolol determined under similar conditions was 11.9 ± 0.8. <sup>c</sup>Solubility and P<sub>e</sub> values are mean (SD) from 3 separate determinations.

Table 4. Antimycobacterial Profiles of Indolecarboxamide 16 and Indolylmethylamine 33

no.	<i>M. tb</i> H37Rv (μM)			<i>M. bovis</i> BCG (μM)				Vero IC <sub>50</sub> (μM) <sup>c</sup>
	MIC <sub>50</sub> <sup>a</sup>	MIC <sub>90</sub> <sup>a</sup>	MBC <sub>99.9</sub> <sup>b</sup>	MIC <sub>50</sub> /MIC <sub>90</sub> in 7H9 media			MBC <sub>99.9</sub> <sup>b</sup>	
				standard media	no glycerol	with 10% FBS		
16	0.02	0.04	0.08	0.08	0.02/0.04	0.01/ <sup>d</sup>	0.02/0.08	>100
33	0.05	0.13	0.63	0.16	0.04/0.08	0.04/ <sup>d</sup>	0.07/0.16	22 ± 2

<sup>a</sup>Lowest concentration required to reduce bacterial growth by 50% (MIC<sub>50</sub>) or 90% (MIC<sub>90</sub>) compared to untreated cultures. MIC<sub>50</sub> and MIC<sub>90</sub> of isoniazid (control) on *M. tb* were 1.8 μM and 3.8 μM. <sup>b</sup>Minimum compound concentration required to kill 99.9% of bacteria. Control isoniazid had MBC<sub>99.9Mtb</sub> of 3.2 μM and MBC<sub>99.9BCG</sub> of 10 μM. <sup>c</sup>Concentration required to reduce growth of mammalian Vero cells by 50% compared to untreated controls. Selectivity indices (IC<sub>50Vero</sub>/MIC<sub>50</sub>, SIs) for 16 was >5000 (*M. tb*, *M. bovis* BCG), and for 33, SI was 366 (*M. tb*) and 550 (*M. bovis* BCG). <sup>d</sup>MIC<sub>90</sub> could not be accurately determined in 7H9 in the absence of glycerol due to poor bacterial growth.

series I. As 33 incorporated features that could enhance solubility, we proceeded to evaluate its aqueous solubility. Other structurally related indolylmethylamines and indolecarboxamides were included for comparison (Table 3). Gratifyingly, we found good solubilities in 33 and indolylmethylamines 7, 31, and 25. These compounds were substantially (~10–40-fold) more soluble than the corresponding carboxamides (4, 14, 16, and 8). Similarly, the methylamines of benzothioindole 47 and benzoselenophene 59 had strikingly better solubilities than the corresponding carboxamides (41, 53). Clearly, the gains in solubility were driven by the presence of the protonatable amino side chain and to a lesser extent by the nature of the heteroaromatic scaffold. However, the polar amino side chain could also repress diffusional flux across an absorptive membrane. Hence, we evaluated the PAMPA permeability coefficient (P<sub>e</sub>) of 33 and other soluble indolylmethylamines (Table 3). Encouragingly, the PAMPA P<sub>e</sub> values of the indolylmethylamines were comparable to propranolol, an intermediate to high permeability control<sup>15</sup> and exceeded that of the carboxamides to varying degrees. Next, we determined the stability of 33 to *in vitro* microsomal degradation. Disappointingly, 33 (half-life 8.2 min, rat microsomes) was more susceptible to breakdown than its carboxamide equivalent 16 (half-life 25.6 min). If the amino side chain of 33 is responsible for its metabolic susceptibility,

structural modifications at this site such as α substitution to delay *N*-dealkylation could serve to minimize degradation.

Next, we profiled 33 for antimycobacterial activity. As summarized in Table 4, 33 retained growth inhibitory activity against *M. tb* but at a 3-fold higher MIC<sub>90</sub> (0.13 μM) than carboxamide 16. Changes in media composition (omission of glycerol, addition of fetal bovine serum) had no discernible effect on MICs. Compound 33 was bactericidal against *M. tb* (MBC<sub>99.9</sub> 0.63 μM) and *M. bovis* BCG (MBC<sub>99.9</sub> 0.16 μM) but not against cultures that were nutrient-deprived or oxygen-deprived (Figures S1 and S2). It displayed high levels of selective toxicity (SI > 100) against *M. bovis* BCG and *M. tb*. In all, 33 was admittedly less potent than the carboxamide 16, but this may be compensated to some degree by its greater solubility and permeability.

MmpL3 is the putative target of several indolecarboxamides,<sup>4,6,9</sup> and here we asked if this critical transporter, which is involved in the mycolation of the cell wall,<sup>16,17</sup> was intercepted by the structurally modified scaffolds of series II–VI. To this end, we raised *M. tb* and *M. bovis* BCG mutants to 16, 33, and the benzothioindolylmethylamine 47. These mutant strains, isolated at a frequency of ~10<sup>-8</sup>/CFU, were at least 5-fold less susceptible than the parental strains to growth inhibition by the test compounds (Table S2). Whole genome sequencing of the mutants identified polymorphisms in the

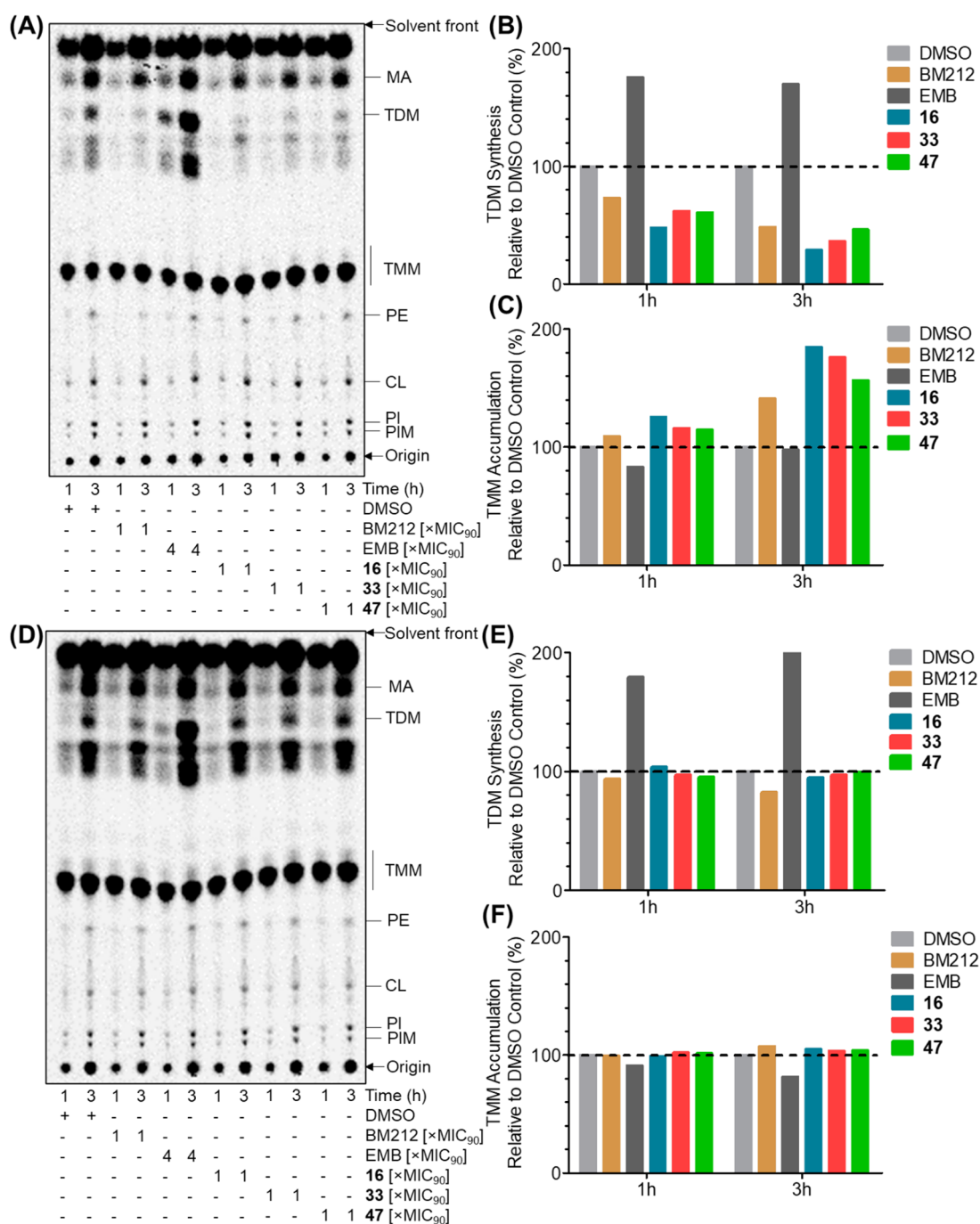


**Figure 2.** (A) Representative TLC of [ $^{14}\text{C}$ ]-labeled lipids extracted from *M. bovis* BCG treated with DMSO, positive control BM212 ( $1 \times \text{MIC}_{90}$ ,  $7.6 \mu\text{M}$ ), negative control ethambutol ( $4 \times \text{MIC}_{90}$ ,  $12.8 \mu\text{M}$ ), and test compounds **16**, **33**, and **47** ( $1 \times \text{MIC}_{90}$ ,  $0.04 \mu\text{M}$ ,  $0.08 \mu\text{M}$ ,  $3.4 \mu\text{M}$ ) at radiolabeling time points 1 h and 3 h. (B) Fraction of TDM in total mycolates (MA+TMM+TDM) in control and drug-treated samples at time points 1 h and 3 h. For each drug-treated sample, the TDM/total mycolates ratio was normalized against the TDM/total mycolates ratio of DMSO control to give %TDM levels relative to DMSO control. (C) Quantification of TMM levels as described for panel B. Descriptions for panels A, B, and C apply to panels D, E, and F, respectively, except that lipids were extracted from the *M. bovis* BCG MmpL3 mutant B47-4. Lipids monitored on the chromatograms were TMM, TDM, mycolic acid (MA), phosphatidylethanolamine (PE), cardiolipin (CL), phosphatidylinositol (PI), and phosphatidylinositol mannoside (PIM). Experiments were repeated twice. One representative result is shown.

*mmpL3* gene, of which the mutations I244F, V285A, and Ins710Q were novel. When some of these MmpL3 mutant strains were tested for cross resistance to other *N*-cyclooctyl analogs (**41**, **53**, **59**), this was duly observed, thus confirming widespread targeting of MmpL3 by these scaffolds (Table S3).

Disruption of MmpL3 activity leads to the accumulation of trehalose monomycolate (TMM) within the cytosol and

concurrent depletion of trehalose dimycolate (TDM) in the cell envelope.<sup>16,17</sup> These changes were monitored in a whole cell [ $^{14}\text{C}$ ]-labeled lipid profiling assay. Briefly, *M. bovis* BCG cultures were treated with test compounds at  $1 \times \text{MIC}_{90}$ , after which newly synthesized lipids were labeled with [ $^{14}\text{C}$ ]acetate at two time points (1 h, 3 h) and extracted for profiling by thin layer chromatography (TLC). A representative TLC profile of

labeled lipids derived from *M. bovis* BCG treated with test compounds (**16**, **33**, **47**), BM212 (MmpL3 inhibitor, positive control), and ethambutol (inhibitor of arabinogalactan synthesis, negative control) is depicted in Figure 2A. Quantification of TDM and TMM levels by densitometry revealed a time-dependent suppression of TDM that coincided with the accumulation of TMM in lipids extracted from cultures treated with **16**, **33**, **47**, and BM212 but not ethambutol (Figure 2B,C). This pattern of change was consistent with MmpL3 inhibition.

Next, the experiment was repeated on one of the *M. bovis* BCG mutants and here the strain B47-4 was selected because its mutation C1932G/F644L was the only recurring polymorphism among the mutants raised against the test compounds. Consistent with the aberration in the *mmpL3* gene sequence, the anticipated changes in TDM and TMM levels were not observed in lipids extracted from B47-4 exposed to BM212, **16**, **33**, and **47** (Figure 2D–F). Similar findings were obtained with **41**, **53**, and **59** (Figure S3). These findings duly recapitulate the MmpL3 inhibitory activities of these compounds.

The ability of MmpL3 to transfer mycolates across the mycobacterial inner membrane is dependent on a functioning proton motive force (PMF), but curiously, inhibition of MmpL3 is not consistently linked to a loss in the PMF.<sup>17–19</sup> In general, direct inhibitors bind to MmpL3 without dissipating the electrical or proton gradient that contributes to the PMF. Indirect MmpL3 inhibitors dissipate the PMF, but the causality of these events remains to be resolved. Having confirmed MmpL3 as a putative target of the short-listed compounds, we proceeded to determine if inhibition was accompanied by a loss in the membrane potential ( $\Delta\Psi$ ) or proton gradient ( $\Delta\text{pH}$ ). Changes in  $\Delta\Psi$  were monitored in *M. bovis* BCG cultures using the fluorescence probe DiOC<sub>2</sub>. Briefly, DiOC<sub>2</sub> fluorescence would change from red to green in cells with depolarized membranes, and declining red/green fluorescence ratios were indicative of losses in  $\Delta\Psi$ . Here we observed a slow decline in the fluorescence ratio of treated cells over time, with pronounced losses observed at time points ( $\geq 12$  h) that coincided with cell death. Hence, it was unlikely that these compounds disrupted the mycobacterial  $\Delta\Psi$  (Figure S4). To determine if the compounds abolished the proton gradient ( $\Delta\text{pH}$ ), we used the radiometric pH indicator BCECF-AM to monitor changes in the intracellular pH of spheroplasts prepared from *M. smegmatis*.<sup>17</sup> Briefly, disruption of  $\Delta\text{pH}$  would acidify the intracellular space within the spheroplasts. This was duly observed in the presence of the protonophore CCCP but not BM212, which inhibited MmpL3 without disrupting the PMF (Table S4).<sup>17</sup> No acidification was also observed in spheroplasts treated with the test compounds. Hence, we concluded that these compounds inhibited MmpL3 without disrupting the PMF.

The incipient indole-2-carboxamide scaffold has yielded several potent bactericidal lead compounds. Here, we showed the feasibility of an amide–amine replacement in retaining potency, as exemplified by the indolylmethylamine **33** (MIC<sub>90Mtb</sub> 0.13  $\mu\text{M}$ ), and importantly, the striking improvement in solubility elicited by this modification. The solubility advantage persisted even when indole was replaced by the more lipophilic benzothiophene and benzoselenophene scaffolds, but overall only the indoles displayed compelling potencies. Second, the indolylmethylamines displayed favorable solubility and PAMPA  $P_e$  profiles but were more

susceptible to microsomal breakdown than the indolecarboxamides. Third, the remarkable activity advantage of the *N*-cyclooctyl ring was consistently observed in the carboxamides of all scaffolds, but it was only evident when attached to the methylamine N of indole. Lastly, the interception of MmpL3 was consistently observed among potent analogs drawn from the different heteroaromatic rings.

## ■ ASSOCIATED CONTENT

### Supporting Information

The Supporting Information is available free of charge at <https://pubs.acs.org/doi/10.1021/acsmmedchemlett.0c00588>.

Synthesis, characterization, and purity determinations of synthesized compounds, NMR spectra of **16** and **33**, MIC, MBC, Vero cell viability, PAMPA  $P_e$ , solubility, microsomal stability, and PMF determinations, mutant selection, and lipid profiling (PDF)

## ■ AUTHOR INFORMATION

### Corresponding Authors

Mei-Lin Go – Department of Pharmacy, National University of Singapore, 117543, Singapore; [orcid.org/0000-0003-4757-3343](https://orcid.org/0000-0003-4757-3343); Phone: +65-65162654; Email: [phagoml@nus.edu.sg](mailto:phagoml@nus.edu.sg)

Yulin Lam – Department of Chemistry, National University of Singapore, 117543, Singapore; [orcid.org/0000-0003-0984-9492](https://orcid.org/0000-0003-0984-9492); Phone: +65-65162688; Email: [chmlamyl@nus.edu.sg](mailto:chmlamyl@nus.edu.sg)

### Authors

Yu Jia Tan – Department of Chemistry, National University of Singapore, 117543, Singapore

Ming Li – Department of Pharmacy, National University of Singapore, 117543, Singapore

Gregory Adrian Gunawan – Department of Chemistry, National University of Singapore, 117543, Singapore

Samuel Agyei Nyantakyi – Department of Pharmacy, National University of Singapore, 117543, Singapore

Thomas Dick – Center for Discovery and Innovation, Hackensack Meridian Health, Hackensack Meridian School of Medicine, Nutley, New Jersey 07110, United States; Department of Microbiology and Immunology, Georgetown University, Washington, D.C. 20057, United States

Complete contact information is available at: <https://pubs.acs.org/10.1021/acsmmedchemlett.0c00588>

### Author Contributions

<sup>‡</sup>Y.J.T. and M.L. are joint first authors. All authors made equal contributions.

### Notes

The authors declare no competing financial interest.

## ■ ACKNOWLEDGMENTS

This work was funded by the Ministry of Education (MoE) Academic Research Fund Grants R148000234114 and R148000286114 to M.L.G., Ministry of Health National Medical Research Council Grant NMRC/TCR/011-NUHS/2014 (Singapore), and the National Institute of Allergy and Infectious Diseases of the National Institutes of Health (USA) Grant R01AI132374 to T.D. The content is solely the responsibility of the authors and does not necessarily represent the official views of the NIH. The authors gratefully

acknowledge MoE Singapore for scholarships to Y.J.T., M.L., and S.A.N., Prof. S. S. Chng and lab members of NUS Chemistry, Prof. N Paton, and the BSL3 core facility of NUHS.

## REFERENCES

- (1) World Health Organization. *Global Tuberculosis Report 2020*; World Health Organization, Geneva, 2020.
- (2) Kondreddi, R. R.; Jiricek, J.; Rao, S. P. S.; Lakshminarayana, S. B.; Camacho, L. R.; Rao, R.; Herve, M.; Bifani, P.; Ma, N. L.; Kuhen, K.; Goh, A.; Chatterjee, A. K.; Dick, T.; Diagana, T. T.; Manjunatha, U. H.; Smith, P. W. Design, Synthesis, and Biological Evaluation of Indole-2- Carboxamides: A Promising Class of Antituberculosis Agents. *J. Med. Chem.* **2013**, *56*, 8849–8859.
- (3) Ballell, L.; Bates, R. H.; Young, R. J.; Alvarez-Gomez, D.; Alvarez-Ruiz, E.; Barroso, V.; Blanco, D.; Crespo, B.; Escibano, J.; González, R.; Lozano, S.; Huss, S.; Santos-Villarejo, A.; Martín-Plaza, J. J.; Mendoza, A.; Rebollo-Lopez, M. J.; Remuñan-Blanco, M.; Lavandera, J. L.; Pérez-Herran, E.; Gamo-Benito, F. J.; García-Bustos, J. F.; Barros, D.; Castro, J. P.; Cammack, N. Fueling Open-Source Drug Discovery: 177 Small-Molecule Leads Against Tuberculosis. *ChemMedChem* **2013**, *8*, 313–321.
- (4) Rao, S. P. S.; Lakshminarayana, S. B.; Kondreddi, R. R.; Herve, M.; Camacho, L. R.; Bifani, P.; Kalapala, S. K.; Jiricek, J.; Ma, N. L.; Tan, B. H.; Ng, S. H.; Nanjundappa, M.; Ravindran, S.; Seah, P. G.; Thayalan, P.; Lim, S. H.; Lee, B. H.; Goh, A.; Barnes, W. S.; Chen, Z.; Gagaring, K.; Chatterjee, A. K.; Pethe, K.; Kuhen, K.; Walker, J.; Feng, G.; Babu, S.; Zhang, L.; Blasco, F.; Beer, D.; Weaver, M.; Dartois, V.; Glynn, R.; Dick, T.; Smith, P. W.; Diagana, T. T.; Manjunatha, U. H. Indolecarboxamide Is a Preclinical Candidate for Treating Multidrug-Resistant Tuberculosis. *Sci. Transl. Med.* **2013**, *5*, 214ra168.
- (5) Onajole, O. K.; Pieroni, M.; Tipparaju, S. K.; Lun, S.; Stec, J.; Chen, G.; Gunosewoyo, H.; Guo, H.; Ammerman, N. C.; Bishai, W. R.; Kozikowski, A. P. Preliminary Structure-Activity Relationships and Biological Evaluation of Novel Antitubercular Indolecarboxamide Derivatives Against Drug-Susceptible and Drug-Resistant Mycobacterium Tuberculosis Strains. *J. Med. Chem.* **2013**, *56*, 4093–4103.
- (6) Lun, S.; Guo, H.; Onajole, O. K.; Pieroni, M.; Gunosewoyo, H.; Chen, G.; Tipparaju, S. K.; Ammerman, N. C.; Kozikowski, A. P.; Bishai, W. R. Indoleamides Are Active Against Drug-Resistant Mycobacterium Tuberculosis. *Nat. Commun.* **2013**, *4*, 2907.
- (7) Stec, J.; Onajole, O. K.; Lun, S.; Guo, H.; Merenbloom, B.; Vistoli, G.; Bishai, W. R.; Kozikowski, A. P. Indole-2-Carboxamide-Based MmpL3 Inhibitors Show Exceptional Antitubercular Activity in an Animal Model of Tuberculosis Infection. *J. Med. Chem.* **2016**, *59*, 6232–6247.
- (8) Lun, S.; Tasneen, R.; Chaira, T.; Stec, J.; Onajole, O. K.; Yang, T. J.; Cooper, C. B.; Mdluli, K.; Converse, P. J.; Nuernberger, E. L.; Raj, V. S.; Kozikowski, A.; Bishai, W. R. Advancing the Therapeutic Potential of Indoleamides for Tuberculosis. *Antimicrob. Agents Chemother.* **2019**, *63*, e00343-19.
- (9) Zhang, B.; Li, J.; Yang, X.; Wu, L.; Zhang, J.; Yang, Y.; Zhao, Y.; Zhang, L.; Yang, X.; Yang, X.; Cheng, X.; Liu, Z.; Jiang, B.; Jiang, H.; Guddat, L. W.; Yang, H.; Rao, Z. Crystal Structures of Membrane Transporter MmpL3, an Anti-TB Drug Target. *Cell* **2019**, *176*, 636–648.
- (10) Caron, G.; Kihlberg, J.; Ermondi, G. Intramolecular Hydrogen Bonding: An Opportunity for Improved Design in Medicinal Chemistry. *Med. Res. Rev.* **2019**, *39*, 1707–1729.
- (11) Ravinder, B.; Rajeswar Reddy, S.; Panasa Reddy, A.; Bandichhor, R. Amide Activation by TMSCl: Reduction of Amides to Amines by LiAlH<sub>4</sub> Under Mild Conditions. *Tetrahedron Lett.* **2013**, *54*, 4908–4913.
- (12) Niculescu-Duvaz, D.; Niculescu-Duvaz, I.; Suijkerbuijk, B. M. J. M.; Ménard, D.; Zambon, A.; Davies, L.; Pons, J.-F.; Whittaker, S.; Marais, R.; Springer, C. J. Potent BRAF kinase inhibitors based on 2,4,5-trisubstituted imidazole with naphthyl and benzothiophene 4-substituents. *Bioorg. Med. Chem.* **2013**, *21*, 1284–1304.
- (13) Dubey, R.; Lee, H.; Nam, D.; Lim, D. Mild Generation of Selenolate Nucleophiles by Thiol Reduction of Diselenides: Convenient Syntheses of Selenyl-Substituted Aryl Aldehydes. *Tetrahedron Lett.* **2011**, *52*, 6839–6842.
- (14) Zhao, Q.; Qian, C.; Chen, X.-Z. Investigation on the One-Step Preparation of 2-Substituted Benzo[B]Thiophenes. *Phosphorus, Sulfur Silicon Relat. Elem.* **2013**, *188*, 873–878.
- (15) Sugano, K.; Hamada, H.; Machida, M.; Ushio, H. High throughput prediction of oral absorption: Improvement of the composition of the lipid solution used in parallel artificial membrane permeability assay. *J. Biomol. Screening* **2001**, *6*, 189–196.
- (16) Grzegorzewicz, A. E.; Pham, H.; Gundi, V. A. K. B.; Scherman, M. S.; North, E. J.; Hess, T.; Jones, V.; Gruppo, V.; Born, S. E. M.; Korduláková, J.; Chavadi, S. S.; Morisseau, C.; Lenaerts, A. J.; Lee, R. E.; McNeil, M. R.; Jackson, M. Inhibition of Mycolic Acid Transport Across the Mycobacterium Tuberculosis Plasma Membrane. *Nat. Chem. Biol.* **2012**, *8*, 334–341.
- (17) Xu, Z.; Meshcheryakov, V. A.; Poce, G.; Chng, S. MmpL3 Is the Flippase for Mycolic Acids in Mycobacteria. *Proc. Natl. Acad. Sci. U. S. A.* **2017**, *114*, 7993–7998.
- (18) Li, W.; Upadhyay, A.; Fontes, F. L.; North, E. J.; Wang, Y.; Crans, D. C.; Grzegorzewicz, A. E.; Jones, V.; Franzblau, S. G.; Lee, R. E.; Crick, D. C.; Jackson, M. Novel Insights into the Mechanism of Inhibition of MmpL3, a Target of Multiple Pharmacophores in Mycobacterium Tuberculosis. *Antimicrob. Agents Chemother.* **2014**, *58*, 6413–6423.
- (19) Li, W.; Stevens, C. M.; Pandya, A. N.; Darzynkiewicz, Z.; Bhattarai, P.; Tong, W.; Gonzalez-Juarrero, M.; North, E. J.; Zgurskaya, H. I.; Jackson, M. Direct Inhibition of MmpL3 by Novel Antitubercular Compounds. *ACS Infect. Dis.* **2019**, *5*, 1001–1012.